A Novel Ganglioside Isolated from Renal Cell Carcinoma

THE JOURNAL OF BIOLOGICAL CHEMISTRY
Vol. 276, No. 20, Issue of May 18, pp. 16695–16703, 2001

Printed in U.S.A.

A Novel Ganglioside Isolated from Renal Cell Carcinoma*

Received for publication, December 29, 2000, and in revised form, February 20, 2001
Published, JBC Papers in Press, February 27, 2001, DOI 10.1074/jbc.M011791200

Akihiro Ito‡, Steven B. Levery§, Seiichi Saito¶, Makoto Satoh¶, and Sen-itiroh Hakomori‡‖

From the ‡Division of Biomembrane Research, Pacific Northwest Research Institute and the Departments of Pathobiology and Microbiology, University of Washington, Seattle, Washington 98122, the §Complex Carbohydrate Research Center, University of Georgia, Athens, Georgia 30602, and the ¶Department of Urology, Tohoku University School of Medicine, Seiryo-machi, Aoba-ku, Sendai 980-8574, Japan

In renal cell carcinoma (RCC), the level of higher gangliosides is correlated with degree of metastatic potential, and cell lines derived from metastatic deposits of RCC are characterized by high expression of disialogangliosides (Saito, S., Orikasa, S., Ohyama, C., Satoh, M., and Fukushi, Y. (1991) *Int. J. Cancer* 49, 329–334 and Saito, S., Orikasa, S., Satoh, M., Ohyama, C., Ito, A., and Takahashi, T. (1997) *Jpn. J. Cancer Res.* (*Gann*) 88, 652–659). We now report two disialogangliosides, G1 and G2, found in the RCC cell line TOS-1. G1 from TOS-1 cells was characterized as having a novel hybrid structure between ganglio-series (region I as in Structure I; same as the terminal structure of ganglioside GM2), and the lacto-series type 1 (region II). The characterization was based on reactivity with various monoclonal antibodies (mAbs) with defined epitope specificity, as well as monosaccharide and fatty acid component analysis, ^{1}H NMR spectroscopy, and electrospray ionization mass spectrometry of the intact compound. G1 showed strong reactivity with mAb RM2, raised originally against TOS-1 cells, and weak cross-reactivity with anti-GM2 mAb MK-1–8. The antigen is hereby termed GalNAc disialosyl Lc_4Cer ($IV^4GalNAcIV^3NeuAcIII^6NeuAcLc_4$; abbreviated $GalNAcDSLc_4$).

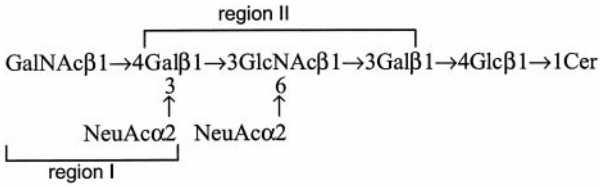

STRUCTURE I

G2 was identified by ^{1}H NMR and mass spectrometry as having a structure similar to Structure I but without the GalNAcβ1→4 substitution and showed strong reactivity with mAb FH9 reported previously to be specific for disialosyl lacto-series type 1 (disialosyl Lc_4) having vicinal α2→3 and α2→6 sialosyl residues, an antigen associated with human colonic cancer. Clinicopathological studies indicate that expression of these disialoganglioside antigens in RCC tissue is correlated with the metastatic potential of RCC.

The expression pattern of glycosphingolipid (GSL)[1] at the tumor cell surface may define the ability of the tumor cell to interact with specific target cell where the GSL antigen is recognized and may thus promote distant metastasis through the blood circulatory or lymphatic system. This general idea is supported particularly by tumor cell adhesion to E-selectin expressed on activated endothelial cells. This process is mediated by the E-selectin epitope expressed on tumor cells, which was identified as either sialosyl-Le^x (SLe^x), sialosyl-Le^a (SLe^a), or their analogs (for review, see Refs. 1–3).

An initial study of GSL patterns of renal cell carcinoma (RCC) and its metastatic deposits indicated that enhanced expression of higher gangliosides having TLC mobility similar to or slower than that of GM2 in original RCC tissue is correlated with metastatic potential (4). However, expression of SLe^x and dimeric Le^x in RCC is higher in differentiated than in undifferentiated form and is not correlated with RCC metastasis (5, 6). This trend is opposite to that in other types of cancer (see above).

Two RCC cell lines derived from its metastatic deposits, TOS-1 and ACHN, are characterized by high expression of disialogangliosides in addition to GM2 but do not express SLe^x or SLe^a (7). Therefore, an unknown mechanism mediated by glycoepitopes different from SLe^x, SLe^a, or their analogs should be considered for RCC metastasis (7). In immunohistological (8) and clinicopathological (9) studies using a series of mAbs directed to di- and monosialogangliosides of RCC, positive staining with these antibodies in original RCC tissue was correlated with later incidence of metastasis.

Disialosylgalactosylgloboside (DSGG) was identified previously as one of the major disialogangliosides from RCC tissues (10). However, further studies indicated that two other novel disialogangliosides are found in RCC tissue as well as TOS-1 cells, and that DSGG is the major disialoganglioside of ACHN but is absent from TOS-1 (see "Discussion"). We report here that the two major disialogangliosides (G1 and G2) present in TOS-1 cells and RCC are not DSGG but have entirely different properties. Their structures were characterized by ^{1}H NMR spectroscopy and electrospray ionization mass spectrometry of intact compounds. G1 is identified as a novel, hybrid structure between ganglio-series and lacto-series type 1, characterized by strong reactivity with mAb RM2, raised originally against TOS-1 cells, and by weak cross-reactivity with anti-GM2 mAb

* This study was supported by NCI, National Institutes of Health (NIH) Grants CA80054 and CA82167 (to S. H.) and the NIH Resource for Complex Biomedical Carbohydrates, P41 RR005351 (to S. B. L.). The costs of publication of this article were defrayed in part by the payment of page charges. This article must therefore be hereby marked "*advertisement*" in accordance with 18 U.S.C. Section 1734 solely to indicate this fact.

‖ To whom correspondence should be addressed. Tel.: 206-726-1222; Fax: 206-726-1212; E-mail: hakomori@u.washington.edu.

[1] The abbreviations used are: GSL, glycosphingolipid; DSGG, disialosylgalactosylgloboside (NeuAcα3Galβ3[NeuAcα6]GalNAcβ3Galα4Galβ4GlcCer); $DSLc_4$, $IV^3NeuAcIII^6NeuAcLc_4$; $GalNAcDSLc_4$, $IV^4GalNAcIV^3NeuAcIII^6NeuAcLc_4$; mAb, monoclonal antibody; MSGG, monosialosylgalactosylgloboside (NeuAcα3Galβ3GalNAcβ3Galα4Galβ4GlcCer); PBS, Dulbecco's phosphate-buffered saline; RCC, renal cell carcinoma (derived mainly from proximal tubular epithelia of kidney); SLe^a, sialosyl-Le^a (NeuAcα3Galβ3[Fucα4]GlcNAcβ3Galβ4Glc); SLe^x, sialosyl-Le^x (NeuAcα3Galβ4[Fucα3]GlcNAcβ3Galβ4Glc); cer, ceramide.

MK-1–8. G2 has the same lacto-series type 1 chain,[2] with a vicinal disialosyl residue, and is identical to the structure described previously as a colonic cancer-associated antigen defined specifically by mAb FH9 (11). In this study, we describe isolation and detailed characterization of G1 and G2 and discuss the possible relationship of their expression to RCC malignancy.

MATERIALS AND METHODS

Cells—TOS-1 was derived from back metastatic lesion of an RCC patient (8). ACHN was purchased from American Tissue Culture Collection (ATCC) and was originally derived from malignant pleural effusion of a patient with widely metastatic RCC. These cells were maintained in high glucose Dulbecco's modified Eagle's medium (Irvine Scientific, Santa Ana, CA) supplemented with 10% fetal bovine serum (Hyclone, Logan, UT), 1 mM sodium pyruvate, 100 IU/ml penicillin G, and 100 μg/ml streptomycin under a humidified atmosphere with 5% CO_2 at 37 °C.

Monoclonal Antibodies—RM2 was established using TOS-1 cells (10), and FH9 was established in our laboratory (11). The anti-GM2 antibody MK1–8 was kindly donated by Dr. Reiji Kannagi (Molecular Pathology, Aichi Cancer Center, Nagoya, Japan).

Extraction of Glycolipids—Glycolipids were extracted from packed cells as described previously (12). Briefly, ~130 ml of packed cells were extracted by homogenization and filtration with 15 volumes of isopropyl alcohol/hexane/water (55:25:20, v/v/v). The extraction/filtration procedure was repeated once more. Combined extracts were evaporated and divided into the upper and the lower phases by Folch's partition (13). The upper phase was dialyzed against distilled water, dissolved in chloroform/methanol/water (30:60:8), and fractionated by DEAE-Sephadex A25 column chromatography into neutral glycolipids and gangliosides. Gangliosides were further separated into mono-, di-, and trisialosyl fractions by stepwise elution with 0.03, 0.13, and 0.45 M ammonium acetate in chloroform/methanol/water (30:60:8). The eluted gangliosides were dialyzed against distilled water and lyophilized. Each fraction was spotted onto a HPTLC plate (Whatman HPKF, Clifton, NJ), developed in a solvent system of chloroform-methanol-0.5% aqueous $CaCl_2$ (50:40:10), and visualized by spraying with 0.5% orcinol in 2 N sulfuric acid.

Purification of Gangliosides—Gangliosides were separated on preparative HPTLC. 50 μl of sample were streaked across a HPTLC plate, developed in a solvent system of chloroform-methanol-0.2% aqueous $CaCl_2$ (50:50:10), and visualized by spraying with 0.001% primulin in acetone/water (4:1). Bands were marked with a pencil under UV light. Marked bands were scraped from the plate using a razor blade, and gangliosides were extracted from the silica by sonicating for 20 min in isopropyl alcohol/hexane/water (55:25:20). The silica was removed by centrifuging at 1000 × *g* for 10 min, re-extracted as above, and the combined supernatants were dried under N_2.

TLC Immunostaining—Immunostaining was performed on HPTLC plates by a modified version of Magnani's procedure (14). Gangliosides were applied on HPTLC plates for chromatography using a solvent system as described above. Plates were air-dried and immersed in 0.5% poly(isobutyl-metacrylate) in hexane/chloroform (9:1) for 1 min, blocked with 3% bovine serum albumin in PBS for 1 h at room temperature, and reacted for 2 h with mAb at room temperature. Plates were gently washed in PBS, incubated with biotinylated secondary antibody for 1 h, incubated with Vector avidin-biotin solution for 30 min, and stained with 0.05% 3′,3-diaminobenzidine and 0.01% H_2O_2 in 0.05 M Tris-HCl, pH 7.6.

Enzyme-linked Immunosorbent Assay—Purified gangliosides were dissolved in ethanol (40 nmol/ml), and a 50-μl aliquot or its serially diluted solution was added to each well of 96-well flat bottom polystyrene plate (Falcon 3915, Becton Dickinson, NJ), dried at 37 °C, and washed in PBS. Each well was blocked with 3% bovine serum albumin in PBS for 1 h, and reacted with mAb for 1 h at room temperature. Each well was washed extensively in PBS containing 0.05% Tween 20 (T-PBS), and incubated with peroxidase-linked secondary antibody for 30 min at room temperature. After washing in T-PBS, each well was supplemented with 0.05 M citric-acid, pH 4.0 containing 0.5 mg/ml of 2,2′-Azinobis (3-ethylbenzthiazoline-sulfonic acid) (ABTS) (Sigma) and 0.01% H_2O_2, and absorbency of the solution at 630 nm was measured with a microplate reader.

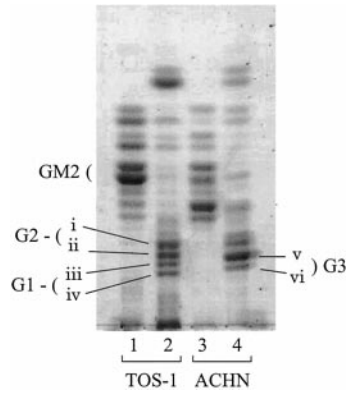

FIG. 1. **HPTLC pattern of TOS-1 and ACHN ganglioside fractions.** Each fraction was spotted onto an HPTLC plate and developed in a solvent system of chloroform-methanol-0.5% aqueous $CaCl_2$ (50:40:10). Bands were revealed by orcinol-sulfuric acid reaction as described under "Materials and Methods." *Lanes 1* and *2*, monosialosyl and disialosyl fractions of TOS-1 gangliosides; *lanes 3* and *4*, monosialosyl and disialosyl fractions of ACHN gangliosides.

Desialosylation of Ganglioside G2—A 70-μg aliquot of ganglioside G2 was desialosylated by heating in 1 ml of isopropyl alcohol/hexane/water (55:25:20, v/v/v; upper phase removed) containing 10% acetic acid in a sealed tube at 100 °C for 4 h. After cooling and drying under a N_2 stream at 35–40 °C, the products were taken up in chloroform/methanol/water (30:60:8 v/v/v; Solvent A) and passed through a ~1-ml column of DEAE-Sephadex A-25 (acetate form, pre-equilibrated with solvent A), washing with 5–6 ml of the same solvent. The combined eluent, free of sialic acid and residual ganglioside, was dried under a N_2 stream and prepared for NMR analysis as described below.

One- and Two-dimensional ^{1}H NMR Spectroscopy—Purified gangliosides (as well as the product from desialosylation of G2) were deuterium exchanged by dissolving in $CDCl_3$-CD_3OD 2:1, evaporating thoroughly under dry nitrogen (repeating 2×), and then dissolved in 0.5 ml of Me_2SO-d_6/2% D_2O (15) for NMR analysis. One-dimensional ^{1}H NMR spectra were acquired at 800 MHz (temperature, 308 K) on a Varian Unity Inova spectrometer, with suppression of the residual HOD signal by a presaturation pulse during the relaxation delay. NMR data were interpreted with comparison to published spectra of related glycosphingolipids (10, 16–23) or to spectra of relevant glycosphingolipid standards acquired under comparable conditions. Two-dimensional ^{1}H–^{1}H-dqCOSY (24, 25), -TOCSY (26, 27), and -NOESY (28) experiments were performed at either 600 or 800 MHz on Varian Unity Inova spectrometers using standard acquisition software available in the Varian VNMR software package.

Glycosyl and Fatty N-Acyl Composition Analysis—Analysis of monosaccharide and fatty acid components were performed by GC/MS (as per-*O*-trimethylsilyl methyl glycosides and methyl esters, respectively) following methanolysis of gangliosides and derivatization according to protocols described in detail elsewhere (29).

Electrospray Ionization Mass Spectrometry—ESI-MS was performed in the positive ion mode on a PE-Sciex (Concord, Ontario, Canada) API-III spectrometer, with a standard IonSpray source, using direct infusion (3–5 μl/min) of ganglioside samples dissolved (~20 ng/μl) in 100% MeOH (orifice-to-skimmer voltage [OR], 130 V; Ionspray voltage, 5 kV; interface temperature, 45 °C) (29). Fragment nomenclature is after Costello and co-workers (30, 31) as modified by Adams and Ann (32).

RESULTS

Disialoganglioside Pattern of RCC Cell Lines TOS-1 and ACHN—Four major disialoganglioside component bands (i, ii, iii, iv) were separated from TOS-1 cells, and two components (v, vi) were separated from ACHN cells (Fig. 1). mAb RM2 reacted strongly with iii and iv from TOS-1, which are termed G1. The ganglioside corresponding to components i and ii barely reacted with mAb RM2 but reacted strongly with FH9 and is termed G2. Similarly, components v and vi did not react with RM2, but reacted strongly with mAb 5F3, and are termed G3. Thus,

[2] Glycosphingolipids are abbreviated according to the recommendations of the IUPAC-IUB Commission on Biochemical Nomenclature (CBN for lipids: (1977) *Eur. J. Biochem.* **79**, 11–21; (1982) *J. Biol. Chem.* **257**, 3347–3351; and (1987) *J. Biol. Chem.* **262**, 13–18). However, the suffix -OseCer is omitted. Gangliosides are abbreviated according to the extended version of Svennerholm's list (Holmgren *et al.* (1980) *Proc. Natl. Acad. Sci. U. S. A.* **77,** 1947–1950).

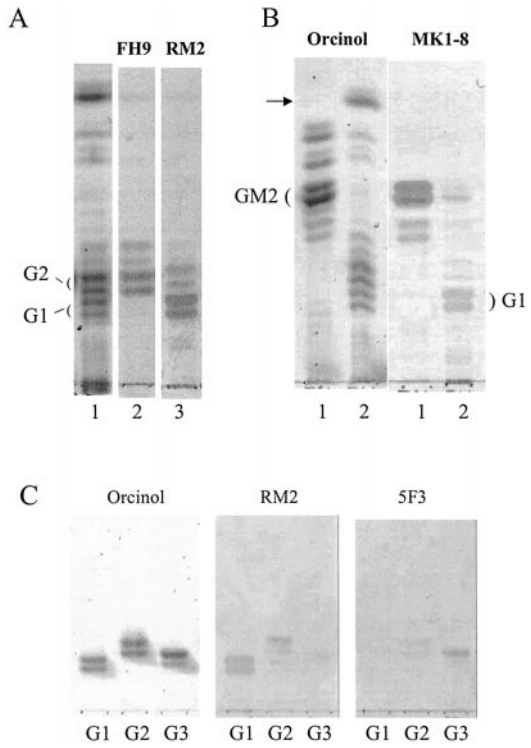

FIG. 2. **TLC immunostaining of TOS-1 and ACHN gangliosides.** HPTLC was developed in a solvent system of chloroform-methanol-0.5% aqueous $CaCl_2$ (50:40:10), and bands were stained with mAbs as described under "Materials and Methods" and compared with patterns from orcinol-sulfuric acid staining. *A*, immunostaining of TOS-1 disialosyl fraction; *lane 1*, orcinol-sulfuric acid; *lane 2*, mAb FH9; *lane 3*, mAb RM2. *B,* monosialosyl (*lane 1*) and disialosyl (*lane 2*) ganglioside fractions of TOS-1 cells. *Left*, orcinol-sulfuric acid; *right*, anti-GM2 mAb MK1–8. *Arrow* indicates sulfatide in orcinol staining of disialosyl fraction. *C,* orcinol-sulfuric acid staining (*left*), mAb RM2 immunostaining (*middle*), and mAb 5F3 immunostaining (*right*) of purified disialogangliosides (G1, G2) from TOS-1 cells and disialoganglioside G3 from ACHN cells.

components i and ii showed the same reactivity with anti-carbohydrate mAbs and were assumed to have the same carbohydrate structure, as was also the case for iii and iv, and v and vi, respectively. These assumptions were confirmed by further studies of each component, which were purified by repeated preparative HPTLC, and subjected to (*a*) detailed immunochemical analysis using various mAbs, and (*b*) detailed chemical analysis by ^{1}H NMR spectroscopy and mass spectrometry, as described under "Materials and Methods." Immunostaining patterns with mAbs RM2, MK-1–8, FH9, and 5F3 of purified G1, G2, and G3 are shown in Fig. 2.

Immunochemical Analysis of Purified G1, G2, and G3—G1 as above was strongly TLC immunostained with mAb RM2, but G2 was barely reactive. G1, but not G2, was stained with anti-GM2 mAb MK-1–8. On the other hand, G2 was strongly stained with mAb FH9, which defines disialosyl type 1 chain (disialosyl Lc_4Cer, *i.e.* $IV^3NeuAcIII^6NeuAcLc_4Cer$) (11), whereas G1 was not stained. Comparative reactivity of various gangliosides and GSLs with RM2 is shown in Fig. 3. These results are consistent with chemical analysis, indicating that G2 is identical to the FH9 antigen and G1 is GalNAc β1→4 linked to the terminal Gal of FH9 antigen.

Disialoganglioside bands v and vi from ACHN cells, defined by mAb 5F3, were identified as DSGG. These results will be described elsewhere, together with reactivity and tissue distribution pattern of the antigen defined by 5F3.

Glycosyl and Fatty N-Acyl Composition Analysis of TOS-1 Gangliosides—Monosaccharides were identified by GC-MS

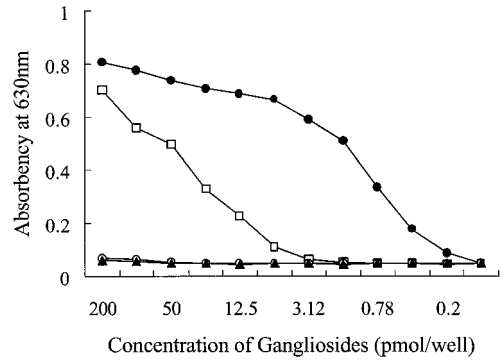

FIG. 3. **Reactivity of mAb RM2 with various gangliosides.** Purified ganglioside was dissolved in ethanol (40 nmol/ml), and serially diluted solution was added to each well of 96-well flat-bottom polystyrene plate, air-dried, and blocked with 3% bovine serum albumin in PBS. RM2 was added to each well and antibody-binding activity was determined by ELISA as described under "Materials and Methods." ●, $GalNAcDSLc_4$ purified from fraction G1; □, $DSLc_4$ purified from fraction G2; ○, DSGG purified from fraction G3; ▲, MSGG, GM2, 2→3 sialosylparagloboside ($IV^3NeuAcnLc_4$), 2→6 sialosylparagloboside ($IV^6NeuAcnLc_4$), SLe^x ($IV^3NeuAcIII^3FucnLc_4$).

analysis of the per-*O*-trimethylsilyl derivatives of methyl glycosides produced from G1 and G2 following methanolysis and re-*N*-acetylation (data not shown). In the analysis of both G1 and G2, derivatives of Glc, Gal, GlcNAc, and NeuAc were identified in 1:2:1:2 ratio, but G1 was distinct from G2 in yielding an additional peak corresponding to a residue of GalNAc. Fatty acids in the ceramides of G1 and G2 were then identified as their methyl esters by GC-MS of hexane extracts of the methanolysates (data not shown). The predominant fatty acids from ganglioside G1 were 16:0, 24:1 (mostly nervonate), and 24:0, together with significant amounts of 18:0 and 22:0, and much smaller amounts of various other species, including 22:1, 18:1 (oleate), 16:1, 26:1, 14:0, 15:0, 23:0, and 26:0. The distribution from G2 was very similar, but with a much higher proportion of 16:0 fatty acid, and with some of the minor species near or below the limits of detection.

One and Two-dimensional ^{1}H NMR Spectroscopy—For structural characterization, high resolution one-dimensional ^{1}H and two-dimensional ^{1}H–^{1}H correlation NMR spectra were acquired at 800 MHz on both TOS-1 gangliosides in Me_2SO-d_6/2% D_2O. One-dimensional ^{1}H NMR spectra of G2 and G1 are reproduced in Fig. 4, *panels A* and *B*, respectively; two-dimensional TOCSY and NOESY spectra of G1 are represented in Fig. 5, *panels A* and *B*; chemical shift data (and $^3J_{1,2}$ coupling constants) are compiled in Table I. The one-dimensional NMR spectrum of the simpler compound, G2, clearly displays two characteristic α-NeuAc H-3eq resonances at 2.769 and 2.727 ppm, as well as four β-anomeric resonances ($^3J_{1,2}$ = 7–9 Hz) in the downfield region, of which that at 4.512 ppm could be tentatively assigned as the β-GlcNAc H-1, that at 4.160 ppm most likely as the β-Glc H-1, and those at 4.248 and 4.117 ppm as two β-Gal H-1, in agreement with the glycosyl composition analysis. Based on analogy to published NMR data, the rather upfield chemical shift of one of the β-Gal H-1 resonances suggested the possibility of a type 1 chain core, as only the terminal β-Gal H-1 of Lc_4Cer has ever been observed upfield of 4.15 ppm (18). Three NAc methyl singlets (1.888, 1.875, and 1.759 ppm) are likewise consistent with the presence of two α-NeuAc and one β-GlcNAc residue in the ganglioside; moreover, the chemical shifts of the two more downfield singlets suggested the presence of NeuAc in both α2→3 and α2→6 linkages, respectively (10, 17, 20). The possibility that the two NeuAc residues are linked together (*i.e.* as a NeuAcα2→8NeuAcα2→X disaccharide structure) appears unlikely, as data previously

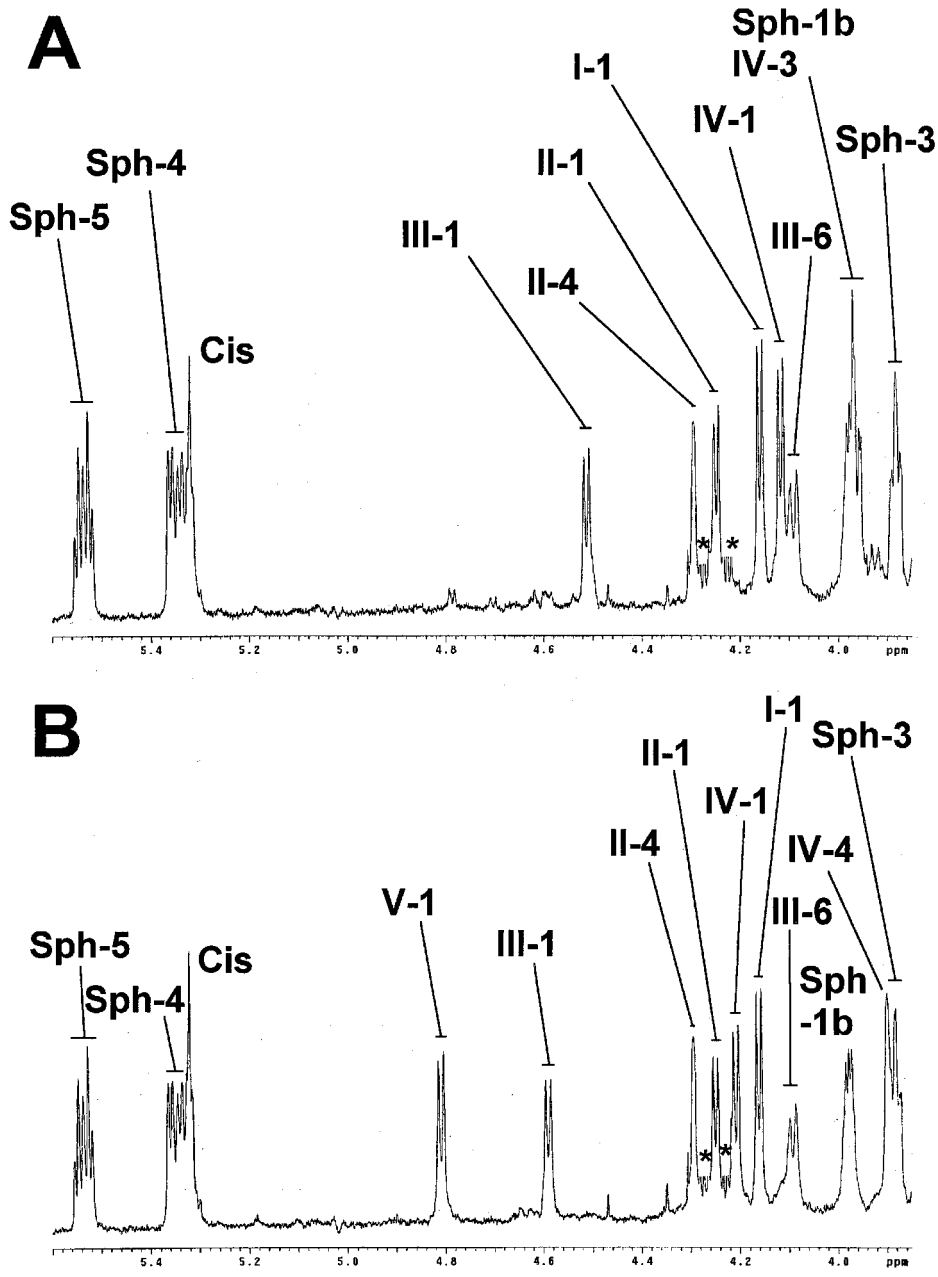

FIG. 4. **Downfield regions (3.85–5.60 ppm) of one-dimensional proton NMR spectra of TOS-1 ganglioside fractions G2 (*A*) and G1 (*B*) in Me_2SO-d_6/D_2O at 308 K.** Arabic numerals refer to ring protons of residues designated by roman numerals for the corresponding glycan sequence starting from β-Glc ≡ I (see Table I). *Sph* refers to protons of the sphingosine backbone; *Cis* refers to vinyl protons of unsaturated fatty-*N*-acyl groups. *Asterisks* mark the location of impurity peaks common to both samples that were deleted for clarity.

published for disialosyl *versus* parent monosialosyl gangliosides (16, 33) shows that attachment of a second NeuAc α2→8 to the first results in substantial shift changes for key resonances of the newly internalized residue, upfield for H-3eq and downfield for H-3ax and H-4. For example, in comparing these resonances in NeuAc A of GD3 *versus* GM3, $\Delta\delta = -0.41, +0.33$, and $+0.28$ ppm, respectively; these changes result in chemical shifts of 2.34, 1.69, and 3.83 ppm, respectively, for these signals in GD3 (33). There are no indications from the data for H-3eq, H-3ax, or H-4 of NeuAc in ganglioside G2 for such shielding/deshielding interactions affecting either of the NeuAc residues. The presence of two other resonances in the downfield region, a broad doublet at 4.091 ppm, and a narrow signal, resembling a β-Gal H-4 in its splitting pattern, but unusually deshielded at 4.293 ppm, are unique features compared with any previously published spectral data.

The spectrum of G1 clearly displays several similar features, in particular the latter two resonances essentially unaffected at 4.091 and 4.294 ppm, respectively. These similarities suggest a close structural relationship between G1 and G2, with the former most likely representing addition of a single monosaccharide residue to the latter. The additional residue is manifested by the appearance of a second downfield β-anomeric resonance tentatively assigned as β-GalNAc H-1. Significant glycosylation-induced shift changes are observable involving the β-Gal H-1 resonance at 4.117 ppm in G2 (apparently shifted to 4.207 ppm in G1), the β-GlcNAc H-1 resonance at 4.512 ppm (shifted to 4.590 ppm in G1), and the α-NeuAc H-3eq resonance at 2.769 (shifted to 2.571 ppm in G1). Changes in chemical shifts of 2 of 3 NAc methyl singlets are also apparent, with those at 1.888 and 1.759 ppm, shifting to 1.871 and 1.793 ppm (coincident with the NAc signal for the β-GalNAc residue), respectively. These suggest the presence in G2 of a terminal NeuAcα2→3Galβ1→3GlcNAcβ1→ trisaccharide to which, in G1, a β-GalNAc has been added in a position to affect resonances of these three residues most strongly. Comparison of the data on G2 and G1 available from two-dimensional NMR analysis shows that the ^1H resonance undergoing the largest change is that for H-4 of the β-Gal correlating with the H-1 at 4.117 in G2 and 4.207 ppm in G1 ($\Delta\delta_{H\text{-}4}$ = 0.3 ppm), suggesting attachment of the GalNAcβ1→4 to this

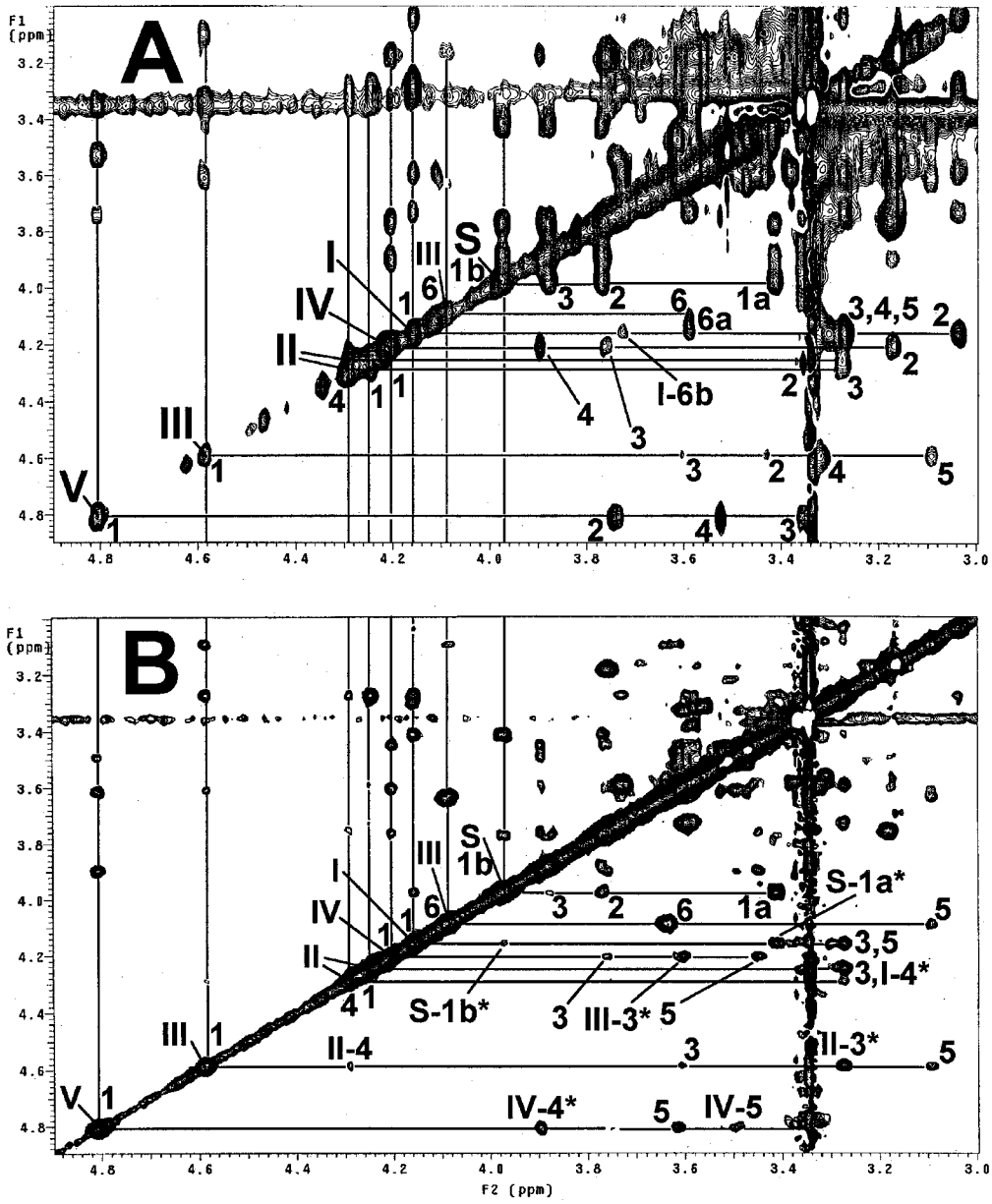

FIG. 5. **Downfield sections (3.00–4.90 ppm) of two-dimensional proton correlation NMR spectra of TOS-1 ganglioside fraction G1 in Me_2SO-d_6/D_2O at 308 K.** *A*, TOCSY (200 ms mixing time); *B*, NOESY (150 ms mixing time). Arabic numerals refer to ring protons of residues designated by roman numerals for the corresponding glycan sequence starting from β-Glc ≡ I (see Table I). *S* refers to protons of the sphingosine backbone. Cross-peak labels marked by *asterisks* in *B* correspond to key interglycosidic NOE correlations, *i.e.* GalNAc V-1/Gal IV-4; Gal IV-1/GlcNAc III-3; GlcNAc III-1/Gal II-3; Gal II-1/Glc I-4; Glc I-1/S-1a, S-1b.

β-Gal in G1. Consistent with this tentative assessment, the chemical shifts of resonances associated with the terminal disaccharide, *i.e.* α-NeuAc H-3eq, H-3ax, H-4, and NAc methyl, β-Gal H-1, along with the newly added β-GalNAc H-1 and NAc methyl, are very similar in G1 to those found for the NeuAcα2→3(GalNAcβ1→4)Galβ1→3 trisaccharide of GM2 ganglioside (16, 21, 34). This supports by analogy that the structural relationship between G2 and G1 is the addition of GalNAcβ1→4 to β-Gal of the terminal NeuAcα2→3Galβ1→3 disaccharide of the former, consistent with the reactivity of G1 but not G2 with anti-GM2 MAb MK-1–8.

Because neither reactivity with antibodies nor analysis of NMR spectra by analogy and chemical shift changes are completely unambiguous indicators of structure, and especially in view of the complexity and novelty of the one-dimensional NMR spectra, further glycosyl connectivity analysis was carried out by acquisition of ^1H–^1H NOESY data (shown for G1 only in Fig. 5, *panel B*), which is an indicator of spatial proximity between nuclei. With few published exceptions (see Ref. 35), the magnitudes of interresidue NOEs are greatest between those nuclei directly connected by glycosyl linkages. In the case of G2, strong interresidue NOEs can be clearly observed between β-Gal H-1 and β-GlcNAc H-3; between β-GlcNAc H-1 and H-3 of the other β-Gal; and between β-Glc H-1 and Cer H-1a/H-1b (an NOE between the internal β-Gal H-1 and the β-Glc residue is somewhat ambiguous, but this linkage is unlikely to be anything but Galβ1→4). These data are consistent with a type 1 chain, Lc_4Cer core structure for G2. Unfortunately, no NOEs were observed between either of the NeuAc residues and those of the core glycan. The reactivity of G2 with MAb FH9, previously shown to react with a disialosyl-Lc_4Cer having NeuAc residues linked α2→3 to Galβ1→3 IV and α2→6 to GlcNAcβ1→3 III, suggests the same structure for this ganglioside, and is certainly consistent with the NMR data. In the

TABLE I

Proton chemical shifts (ppm from tetramethylsilane) and $^3J_{1,2}$ coupling constants (Hz) for TOS-1 gangliosides in dimethylsulfoxide-d_6/2% D_2O at 308 K

	NeuAcα2→6 GalNAcβ1→4 NeuAcα2→3Galβ1→3 A	B	V	GlcNAcβ1→3Galβ1→4Glcβ1→1Cer IV	III	II	I	R
G2[a]								
H-1				4.117	4.512	4.248	4.160	3.421 (a)
($^3J_{1,2}$)				(7.7)	(8.3)	(7.8)	(7.7)	3.972 (b)
H-2				3.276	3.397	3.352	3.037	3.765
H-3	2.769 (eq)	2.727 (eq)		3.962	3.659	3.275	3.307	3.884
	1.346 (ax)	1.255 (ax)						
H-4	3.534	3.511		3.593	3.278	4.293	3.275	5.355
H-5					3.070		3.270	5.549
H-6							3.586 (a)	1.933
							3.724 (b)	
Nac	1.888	1.875			1.759			
G1[a]								
H-1			4.809	4.207	4.590	4.249	4.160	3.414 (a)
($^3J_{1,2}$)			(8.9)	(7.8)	(8.0)	(7.5)	(7.7)	3.977 (b)
H-2			3.742	3.169	3.427	3.356	3.039	3.769
H-3	2.571 (eq)	2.719 (eq)	3.360	3.759	3.605	3.277	3.305	3.878
	1.590 (ax)	1.263 (ax)						
H-4	3.690	3.506	3.526	3.898	3.323	4.294	3.275	5.349
H-5			3.619	3.493	3.095		3.270	5.535
H-6							3.591 (a)	1.933
							3.726 (b)	
Nac	1.874	1.871	1.793		1.793			

[a] G2, G1: purified disialogangliosides from fractions G2 and G1, respectively.

case of G1, the same interresidue NOEs can be observed (including one between the internal β-Gal H-1 and β-Glc H-4); an additional strong NOE is observable between β-GalNAc H-1 and β-Gal IV H-4, again consistent with the GalNAcβ1→4Galβ1→ linkage (Fig. 5, *panel B*).

Final support for the core structure was obtained by acquisition of a one-dimensional NMR spectrum of completely desialosylated G2. The spectrum (not shown) clearly exhibited four β-anomeric resonances at 4.785 ppm ($^3J_{1,2}$ = 8.4 Hz), 4.268 ppm ($^3J_{1,2}$ = 7.7 Hz), 4.168 ppm ($^3J_{1,2}$ = 7.7 Hz), and 4.137 ppm ($^3J_{1,2}$ = 7.2 Hz); additional resonances corresponded to β-Gal II H-4 (3.850 ppm; $^3J_{3,4}$ = 3 Hz)) and β-GlcNAc III NAc (1.815 ppm). These chemical shifts are virtually indistinguishable ($\Delta\delta \leq \pm 0.005$ ppm) from those observed previously for H-1 of β-GlcNAc III, β-Gal II, β-Glc I, β-Gal IV, H-4 of β-Gal II, and NAc of β-GlcNAc III of Lc_4Cer under identical conditions (at 4.781, 4.263, 4.166, 4.136, 3.851, and 1.815 ppm, respectively, Ref. 36; see also Ref. 19), and distinct from spectral data for any other known core structure. Taken together, these data strongly support the structures of G2 and G1 as IV^{3}NeuAc, III^{6}NeuAc-Lc_4Cer and IV^4(β-GalNAc), IV^{3}NeuAc, III^{6}NeuAc-Lc_4Cer, respectively.

Electrospray Ionization Mass Spectrometry—Low resolution ESI mass spectra of both TOS-1 gangliosides were acquired by direct infusion as described previously (29). Single quadrupole mass spectra of G2 and G1 are reproduced in Fig. 6, *panels A* and *B*, respectively; assignments for fragments are summarized in Scheme 1, *a* and *b* (nominal, monoisotopic *m/z* are used throughout). The most abundant molecular adduct ions $[M-2H+3Na]^+$ are observed for G2 (*panel A*) at *m/z* 1875, 1985, and 1987, corresponding to a glycan formula Hex_3·HexNAc·$NeuAc_2$ in combination with ceramides consisting of d18:1 sphingosine predominantly *N*-acylated with 16:0, 24:1, and 24:0 fatty acids. In the spectrum of G1 (*panel B*), the most abundant molecular adduct ions are observed at *m/z* 2078, 2188, and 2190, corresponding to a glycan formula Hex_3·$HexNAc_2$·$NeuAc_2$ in combination with the same predominant ceramides. The additional HexNAc residue observed for G1 is consistent with the glycosyl composition and NMR analysis, and the relative abundances of the molecular species are essentially consistent with the fatty acid analyses, including the greater proportion of the 16:0 species in G2. As often is the case with ESI-MS, the higher molecular weight ganglioside G1 also produces a more abundant set of dicationized doubly charged molecular ions, $[M-2H+4Na]^{2+}$, observed at *m/z* 1050.5, 1105.5, and 1106.5 (*panel B*).

Both gangliosides readily lose 1 and 2 residues of NeuAc (as NeuAc−H+Na), giving abundant sets of Y fragments at *m/z* 1562/1672/1674 and 1249/1359/1361 for G2, and at *m/z* 1765/1875/1877 and 1452/1562/1564 for G1. The latter sets in each case represent double cleavage ions, which might be expected to be of low abundance, but in fact they are more abundant than the losses of single NeuAc residues. An additional loss of 1 HexNAc residue from G1 yields a set of Y fragments identical to that at 1249/1359/1361 observed for G2, and below this mass, the fragmentation patterns are very similar, except for the higher abundance of the 16:0 species in G2. Thus Y_2 (Hex_2Cer) and Y_1 (HexCer) fragments are observable at *m/z* 884/994/996 and 722/832/834 in both spectra, whereas a set of $Y_{3\alpha}$ fragments, which could be expected at *m/z* 1400/1510/1512, is not observed significantly above noise level in either spectrum. $Y_{3\alpha,3\beta}$ fragments at *m/z* 1087/1197/1199 are similarly not observed, although these represent a double cleavage not expected to be very abundant. An interesting double cleavage of one NeuAc residue and the sphingosine moiety at the C2–C3 bond ("G" fragmentation) yields sets of fragments at *m/z* 1325/1435/1437 for G2 (*panel A*) and at *m/z* 1528/1638/1640 for G1 (*panel B*). Such cleavages of the sphingenine C2–C3 bond have been observed previously in positive ion ESI-MS of glycosphingolipids (37, 38).

The fragmentation data are consistent with the proposed structures for G1 and G2, but in the absence of certain ions as mentioned above, they are not unambigous with respect to key parts of their putative sugar sequences. For example, in the absence of an observable set of $Y_{3\alpha}$ fragments, these data would not by themselves rule out the possibility of a disialosyl disaccharide in the structure. However, the presence of such a disialosyl linkage is not consistent with the observed chemical shifts for key NeuAc resonances in the NMR spectra of G2 and G1. Other features of the proposed structures are supported with very high confidence level by the NMR data and are consistent also with the pattern of monoclonal antibody reactivities (G2 with mAb FH9 and G1 with MK-1–8).

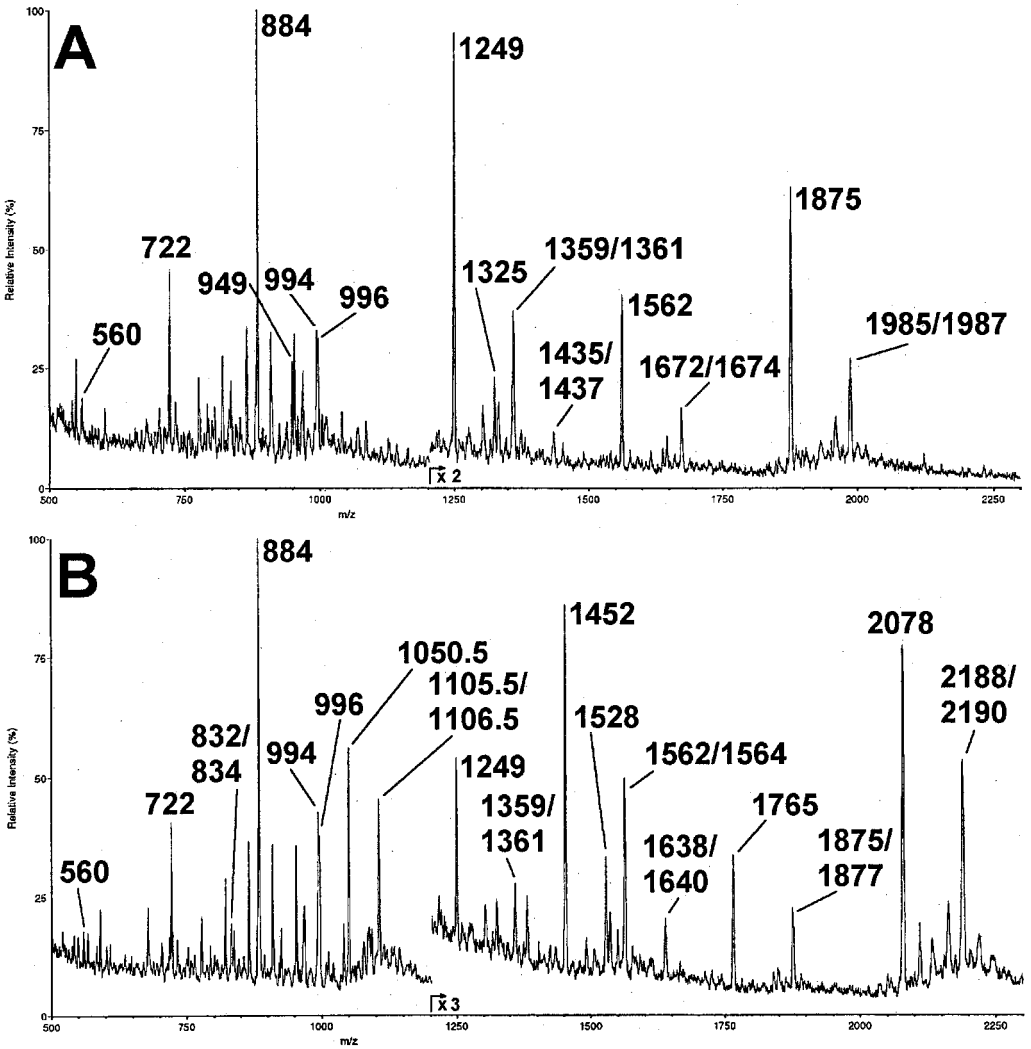

FIG. 6. **Positive ion mode electrospray ionization mass spectra of TOS-1 ganglioside fractions G2 (*A*) and G1 (*B*).** Major sodiated molecular ion adducts $[M-2H+3Na]^+$ (as well as $[M-2H+4Na]^{2+}$ for G1) and key fragments are labeled (nominal, monoisotopic *m/z*). For explanation of fragments, see text and Scheme 1.

DISCUSSION

Many studies indicate that certain GSLs and gangliosides in tumor cells define their malignancy, in terms of metastatic potential (1). Our initial, comparative study on GSL and ganglioside patterns showed enhanced expression of GM2 or gangliosides higher than GM2 (including slow-migrating disialoganglioside species) in RCC having metastatic deposits and in the deposits themselves compared with RCC without metastatic deposits (4). Our subsequent studies were focused on the following: (*a*) establishment of RCC cell lines, and their tumor cell biological properties (8); (*b*) biochemical characterization of major gangliosides showing enhanced expression in RCC tissues, identified as monosialosyl- and disialosylgalactosylgloboside (MSGG and DSGG) (10); (*c*) production of mAb RM2 directed to TOS-1 cells, mAb RM1 directed to RCC (10), and mAb 5F3 directed to RCC gangliosides;[3] and (*d*) application of these antibodies to compare expression of defined epitopes in RCC having metastatic deposits, the deposits themselves, and RCC without metastatic deposits. Expression of each of the antigens defined by RM2, RM1, and 5F3 was correlated with metastatic potential (9).[3] This series of studies indicated that in addition to previously identified DSGG two other disialogangliosides are found as major components of RCC and TOS-1 cells: G1 (defined by mAb RM2) and G2 (defined by mAb FH9). Expression of SLe^x or dimeric Le^x in RCC was found to be correlated with degree of differentiation, but not with metastatic potential (5, 6). In contrast, expression of SLe^x and SLe^a in colorectal carcinoma was highly correlated with metastatic potential (1–3).

Our results clearly identify one major disialoganglioside (G1) expressed in RCC tissue and a cell line derived therefrom (TOS-1) as GalNAc $\beta1\rightarrow4$ linked to terminal Gal of disialosyl Lc_4Cer, and the other disialoganglioside (G2) as disialosyl Lc_4Cer, *i.e.* FH9 antigen reported previously as colonic cancer-associated antigen defined by mAb FH9. Disialoganglioside fraction of RCC tissue in some cases was identified as DSGG, which shows nearly identical TLC mobility, and co-migration in various solvent systems, to that of a novel antigen now identified as $GalNAcDSLc_4$. This novel antigen is a hybrid-type composed of ganglio-series with the same structure as GM2 (region I), and lacto-series type 1 with a vicinal disialosyl residue (region II in Structure I in the Abstract, and Fig. 7). Ganglio-series structures are characterized by $\beta1\rightarrow4$GalNAc linked to Gal, whereas lacto-series are characterized by

[3] A ganglioside from RCC tissue showing the same TLC mobility as G1 (*i.e.* between that of GD1a and GD1b) but not showing reactivity with RM2, was found. mAb 5F3 was prepared against this ganglioside. Immunohistological studies of many cases of RCC, using mAbs RM1, RM2, and 5F3, showed clear correlation between metastatic potential and the epitopes defined by these mAbs (A. Ito, Dr. Med. Sci. (Ph.D. thesis) presented at Tohoku Univ. School of Medicine, Japan, 1997).

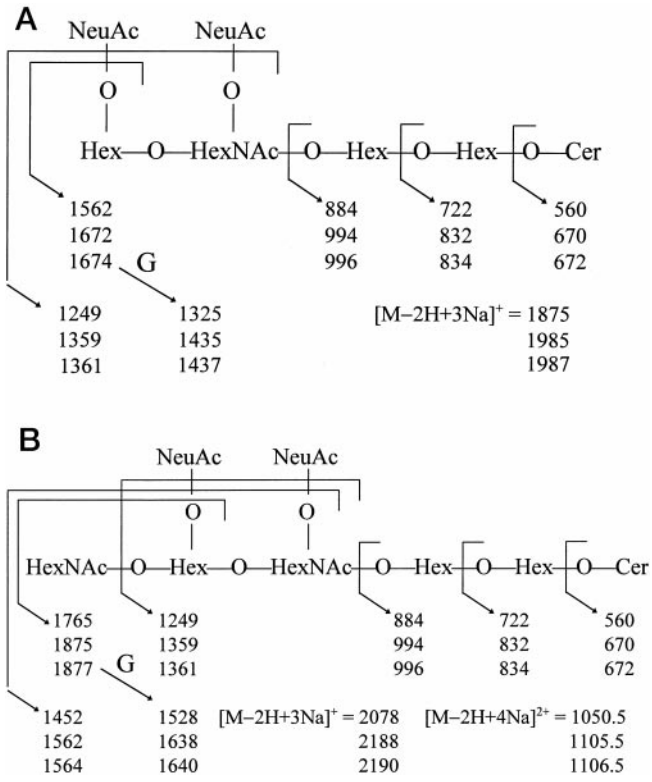

SCHEME 1. **Fragmentation of major sodiated molecular ion adducts for TOS-1 ganglioside fraction G2 (*A*) and G1 (*B*), respectively.**

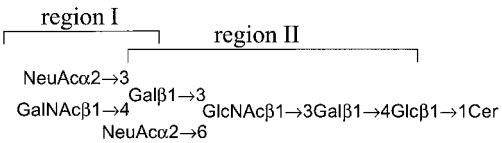

FIG. 7. **Structure of major disialoganglioside of TOS-1 cells and RCC tissues.** *Region I* represents ganglio-series structure, GM2. *Region II* represents lacto-series type 1 structure.

β1→3GlcNAc linked to Gal. These two structures are usually mutually exclusive, and hybrids are rare in humans and mammals. There are two types of ganglio/lacto-series hybrids, branched and linear. The first branched hybrid structure was found in undifferentiated murine leukemia cells, with the structure below, where R_1 could be Galα1→3Galβ1→4 (39).

$$\begin{matrix} R_1\rightarrow GlcNAc\beta1\rightarrow3 \\ R_2\rightarrow GalNAc\beta1\rightarrow4 \end{matrix} Gal\beta1\rightarrow4Glc\beta1\rightarrow1Cer$$

The level of this hybrid structure declined upon differentiation of leukemia cells, and the structure appears to represent undifferentiated state of the cells. A similar branched ganglio/lacto hybrid with R_1 equal to GM2 structure or with R_2 equal to Galβ1→3 structure was isolated from brain of patients with amyotrophic lateral sclerosis-like disorder (22). The first linear-type hybrid GSL was found in the liver of English sole (40), and a similar one was found later in roe of striped mullet (23). GalNAcDSLc$_4$ from G1 fraction as described in the present study is also a linear-type hybrid but is derived from human tissue. Expression of ganglio/lacto hybrid structure is apparently repressed in normal mammalian or human tissues, but increases (*i.e.* is "de-repressed") under pathological conditions. It is possible that specificities of β 1→4GalNAc or β1→3GlcNAc transferases are mutually restricted to the respective substrate structures under normal conditions but lose their restriction under pathological conditions, including cancer. This phenomenon could be caused by subtle changes in the transferase genes, or post-translational modification of the transferases.

Three disialogangliosides are present in RCC tissue. One, expressed in TOS-1 cells, is now identified as GalNAcDSLc$_4$, defined by and reacting strongly with mAb RM2. Another, expressed in ACHN cells is now identified as DSGG, which was previously described as one of the major gangliosides of RCC tissue and is now defined by another mAb (5F3) but not by RM2. The third disialoganglioside, expressed in TOS-1 cells, is now identified as disialosyl Lc$_4$ and is identical to the antigen of mAb FH9, described previously as a colonic cancer-associated antigen (11).

In a previous publication (10), we mistakenly assigned the specificity of mAb RM2 as being directed to DSGG (G3), although RM2 was raised against TOS-1 cells. The mistake may have arisen because of the following: (*a*) disialoganglioside fractions prepared from a few cases of RCC tissue contained DSGG and G1 (GalNAc disialosyl Lc$_4$Cer, abbreviated GalNAcDSLc$_4$) in varying proportions; some RCC tissues contained globo-series structures as major component, whereas others contained ganglio/lacto-series structures as major component; (*b*) DSGG and G1 (GalNAcDSLc$_4$) show identical TLC mobility, *i.e.* co-migrate together in various solvent systems; (*c*) the sample prepared from RCC tissue and used for structural analysis contained DSGG as major component but may have been contaminated with a small quantity of G1 showing reactivity with RM2. We have now clarified that RM2 is directed specifically to G1, whereas another mAB, 5F3, is directed specifically to DSGG.[3] It is possible that RCC tissue expresses high level of G1 in some cases, and DSGG in other cases. Cell lines representing the former and latter situations are TOS-1 and ACHN respectively.

From a clinicopathological and histological point of view, RCC cases expressing either GalNAcDSLc$_4$ or DSGG are highly malignant, and show initiation of lymph node and distant metastasis at an early stage (9). Preferential adherence of TOS-1 cells to lung tissue, determined by Stamper-Woodruff assay, is based on interaction of major disialoganglioside present in TOS-1 with receptor present on perialveolar endothelial cells. This process is strongly inhibited by RM2 (7) and is therefore presumed to be mediated by GalNAcDSLc$_4$, rather than DSGG and its corresponding perialveolar receptor. Interestingly, SLe^x, SLe^a, or their analogs, which bind to E-selectin, are not involved in this process. Studies on the identification of the receptors for both GalNAcDSLc$_4$ and DSGG are essential to understand mechanisms for RCC metastasis and its possible inhibition.

Acknowledgments—We thank Theresa Nguyen for her great efforts in growing a large quantity of TOS-1 and ACHN cells, under the supervision of Dr. Kazuko Handa. We also thank Dr. Stephen Anderson for scientific editing and preparation of the manuscript.

REFERENCES

1. Hakomori, S. (1996) *Cancer Res.* **56,** 5309–5318
2. Brodt, P. (1996) in *Cell Adhesion and Invasion in Cancer Metastasis* (Brodt, P., ed), pp. 167–242, Landes/Springer-Verlag, Austin TX
3. Kannagi, R. (1997) *Glycoconj. J.* **14,** 577–584
4. Saito, S., Orikasa, S., Ohyama, C., Satoh, M., and Fukushi, Y. (1991) *Int. J. Cancer* **49,** 329–334
5. Fukushi, Y., Orikasa, S., Shepard, T., and Hakomori, S. (1986) *J. Urol.* **135,** 1048–1056
6. Fukushi, Y., Ohtani, H., and Orikasa, S. (1989) *J. Natl. Cancer Inst.* **81,** 352–358
7. Satoh, M., Handa, K., Saito, S., Tokuyama, S., Ito, A., Miyao, N., Orikasa, S., and Hakomori, S. (1996) *Cancer Res.* **56,** 1932–1938
8. Satoh, M., Nejad, F. M., Nakano, O., Ito, A., Kawamura, S., Ohyama, C., Saito, S., and Orikasa, S. (1999) *Tohoku J. Exp. Med.* **189,** 95–105
9. Saito, S., Orikasa, S., Satoh, M., Ohyama, C., Ito, A., and Takahashi, T. (1997) *Jpn. J. Cancer Res.*(*Gann*) **88,** 652–659
10. Saito, S., Levery, S. B., Salyan, M. E. K., Goldberg, R. I., and Hakomori, S. (1994) *J. Biol. Chem.* **269,** 5644–5652
11. Fukushi, Y., Nudelman, E. D., Levery, S. B., Higuchi, T., and Hakomori, S. (1986) *Biochemistry* **25,** 2859–2866
12. Stroud, M. R., Handa, K., Salyan, M. E. K., Ito, K., Levery, S. B., Hakomori, S.,

Reinhold, B. B., and Reinhold, V. N. (1996) *Biochemistry* **35,** 758–769
13. Folch, J., Lees, M. B., and Stanley, G. H. S. (1957) *J. Biol. Chem.* **226,** 497–509
14. Magnani, J. L., Smith, D. F., and Ginsburg, V. (1980) *Anal. Biochem.* **109,** 399–402
15. Dabrowski, J., Hanfland, P., and Egge, H. (1980) *Biochemistry* **19,** 5652–5658
16. Koerner, T. A. W. J., Prestegard, J. H., Demou, P. C., and Yu, R. K. (1983) *Biochemistry* **22,** 2676–2687
17. Levery, S. B., Salyan, M. E. K., Steele, S. J., Kannagi, R., Dasgupta, S., Chien, J.-L., Hogan, E. L., van Halbeek, H., and Hakomori, S. (1994) *Arch. Biochem. Biophys.* **312,** 125–134
18. Dabrowski, J., Hanfland, P., Egge, H., and Dabrowski, U. (1981) *Arch. Biochem. Biophys.* **210,** 405–411
19. Holmes, E. H., and Levery, S. B. (1989) *Arch. Biochem. Biophys.* **274,** 14–25
20. Levery, S. B., Nudelman, E. D., Kannagi, R., Symington, F. W., Andersen, N. H., Clausen, H., Baldwin, M., and Hakomori, S. (1988) *Carbohydr. Res.* **178,** 121–144
21. Levery, S. B. (1991) *Glycoconj. J.* **8,** 484–492
22. Nakao, T., Kon, K., Ando, S., Miyatake, T., Yuki, N., Li, Y.-T., Furuya, S., and Hirabayashi, Y. (1993) *J. Biol. Chem.* **268,** 21028–21034
23. DeGasperi, R., Koerner, T. A. W., Quarles, R. H., Ilyas, A. A., Ishikawa, Y., Li, S.-C., and Li, Y.-T. (1987) *J. Biol. Chem.* **262,** 17149–17155
24. Rance, M., Sorensen, O. W., Bodenhausen, G., Wagner, G., Ernst, R. R., and Wüthrich, K. (1983) *Biochem. Biophys. Res. Commun.* **117,** 479–485
25. Piantini, U., Sorensen, O. W., and Ernst, R. R. (1982) *J. Am. Chem. Soc.* **104,** 6800–6801
26. Braunschweiler, L., and Ernst, R. R. (1983) *J. Magn. Reson.* **53,** 521–528
27. Bax, A., and Davis, D. G. (1985) *J. Magn. Reson.* **65,** 355–360
28. States, D. J., Haberkorn, R. A., and Ruben, D. J. (1982) *J. Magn. Reson.* **48,** 286–292
29. Levery, S. B., Toledo, M. S., Straus, A. H., and Takahashi, H. K. (1998) *Biochemistry* **37,** 8764–8775
30. Domon, B., and Costello, C. E. (1988) *Biochemistry* **27,** 1534–1543
31. Costello, C. E., and Vath, J. E. (1990) *Methods Enzymol.* **193,** 738–768
32. Adams, J., and Ann, Q. (1993) *Mass Spectrom. Rev.* **12,** 51–85
33. Ando, S., Yu, R. K., Scarsdale, J. N., Kusunoki, S., and Prestegard, J. H. (1989) *J. Biol. Chem.* **264,** 3478–3483
34. Koerner, T. A. W., Prestegard, J. H., Demou, P. C., and Yu, R. K. (1983) *Biochemistry* **22,** 2687–2690
35. Bush, C. A. (1988) *Bull. Magn. Reson.* **10,** 73–95
36. Amado, M., Almeida, R., Carneiro, F., Levery, S. B., Holmes, E. H., Nomoto, M., Hollingsworth, M. A., Hassan, H., Schwientek, T., Nielsen, P., Bennett, E., and Clausen, H. (1998) *J. Biol. Chem.* **273,** 12770–12778
37. Levery, S. B., Toledo, M. S., Straus, A. H., and Takahashi, H. K. (2000) *Rapid. Commun. Mass Spectrom.* **14,** 551–563
38. Hsu, F.-F., and Turk, J. (2001) *J. Am. Soc. Mass Spectrom.* **12,** 61–79
39. Kannagi, R., Levery, S. B., and Hakomori, S. (1984) *J. Biol. Chem.* **259,** 8444–8451
40. Ostrander, G. K., Levery, S. B., Eaton, H. L., Salyan, M. E. K., Hakomori, S., and Holmes, E. H. (1988) *J. Biol. Chem.* **263,** 18716–18725

A Novel Ganglioside Isolated from Renal Cell Carcinoma

Akihiro Ito, Steven B. Levery, Seiichi Saito, Makoto Satoh and Sen-itiroh Hakomori

J. Biol. Chem. 2001, 276:16695-16703.
doi: 10.1074/jbc.M011791200 originally published online February 27, 2001
